fTable of Contents:

Supplementary Figure Legends

Supplementary Figure 1: (A, B) HEK cells were transfected with PC1-V5 or PC1^{R2220W}-V5 and transduced with XBP1s adenovirus 2 days post transfection. Cells were lysed and analyzed 24 hours later by immunoblotting against V5 to detect PC1-CTF and PC1-FL. Anti-XBP1s shows expression in transduced cells, and Hsp90 serves a loading control. (A) and (B) are independent experiments (with 3 independent samples for the PC1-R2220W +/- XBP1s groups) showing reproducibility of the XBP1s effect on PC1^{R2220W} steady-state levels in vitro.

Supplementary Figure 2: Whole kidney panel showing all the sections used in the comparison among the *Pkd1*$^{R2216W/+}$, *Pkd1*$^{R2216W/flox}$*;Pkhd1Cre*, and *Pkd1*$^{R2216W/flox}$*;ROSA-XBP1s;Pkhd1Cre* groups. f, female; m, male. Size bar, 2 mm.

Supplementary Figure 3: Proteasomal inhibition via MG132 treatment leads to an increase in the PC1-CTF levels in PC1^{R2216W}-V5 cells as compared with the untreated cells.

Supplementary Figure 4: (A), IMCD3 *Pkd1*$^{-/-}$ cells were transiently transfected with PC1-V5 or PC1^{R2220W}-V5 mutant. While wild-type PC1-V5 is seen in cilia via anti-V5 staining (co-localizing with the cilia marker Arl13b), the mutant PC1^{R2220W}-V5 is almost undetectable in cilia. Size bar, 2.5 um. (B), Lower magnification view of cells described in (A). PC1-V5 was detected in 48 out of 50 cilia analyzed. On the other hand, PC1^{R2220W}-V5 was found in 1/50 cilia assessed. Size bar, 10 um.

Supplementary Figure 5: (A), 4-PBA enhances trafficking of the PC1^{R2216W} mutant. As seen in figure 4 and recapitulated here, while the PC1$^{V5/+}$ cells display robust ciliary V5 staining (which co-localized with the ciliary marker Arl13b; arrowheads), the PC1$^{R2216W/-}$ mutant displays very low ciliary V5 immunoreactivity. Interestingly, in the presence of 4-PBA (1mM, 48 hours treatment), a partial rescue of the ciliary V5 signal is

observed (indicated by arrowheads). (B), Quantification of the results depicted in (A). Percent positive V5 in cilia (together with absolute values) is shown for *Pkd1*$^{V5/+}$ (122 V5 positive out of 160 cilia quantified), *Pkd1*$^{R2216W/-}$ (12/109), and *Pkd1*$^{R2216W/-}$ + 4-PBA (41/110). Scale bar, 10 um.

Supplementary Figure 6: *Pkd2-BAC* leads to a partial rescue of the cystic phenotype on the *Pkd1*$^{R2216W/flox}$*; Pkhd1Cre* background. (A), Representative images of kidneys with the genotypes indicated by the colored shapes at P24. Scale bar 2 mm. (B, C), Aggregate data from mice with the genotypes indicated by the color codes from (A) at P24 showing significant reversal in kidney weight/body weight ratio (KW/BW) and BUN levels in the presence of *Pkd2-BAC*; ***P< 0.001; **P< 0.01; *P< 0.05. Comparisons among groups were performed using one-way ANOVA followed by Tukey's multiple group comparison post-test.

Supplementary Figure 7: Whole kidney panel showing all the kidneys used in the comparison among the *Pkd1*$^{R2216W/+}$, *Pkd1*$^{R2216W/flox}$*; Pax8*$^{rtTA;}$*tet-OCre*, and *Pkd1*$^{R2216W/flox}$*; Pax8*$^{rtTA;}$*tet-OCre;ROSA-XBP1s* groups. Genders for the experimental groups are indicated adjacent to each section. Size bar, 2mm.

Supplementary Figure 8: (A), Gender comparison of KW/BW ratios among the *Pkd1*$^{R2216W/flox}$*; Pax8*$^{rtTA;}$*tet-OCre;* mice. (B), Comparison of KW/BW ratio for female only *Pkd1*$^{R2216W/flox}$*; Pax8*$^{rtTA;}$*tet-OCre* and *Pkd1*$^{R2216W/flox}$*; Pax8*$^{rtTA;}$*tet-OCre; ROSA-XBP1s* mice. Results are shown as mean ± SEM (Student's t-test); ns, P=0.41; *P=0.02

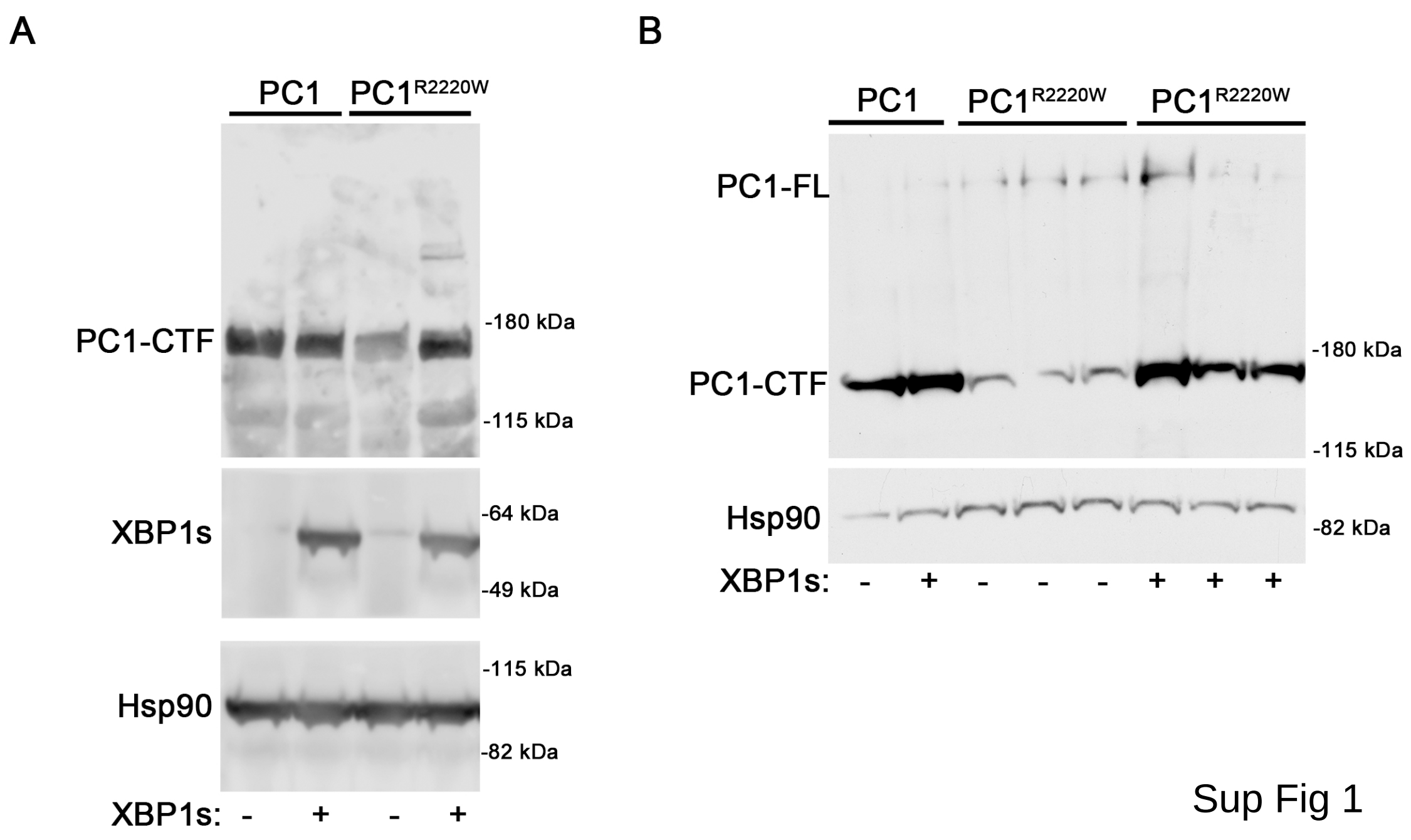
A
PC1
PC1R2220W
PC1-CTF
-180 kDa
-115 kDa
XBP1s
-64 kDa
-49 kDa
Hsp90
-115 kDa
-82 kDa
XBP1s: - + - +
B
PC1
PC1R2220W
PC1R2220W
PC1-FL
PC1-CTF
-180 kDa
-115 kDa
Hsp90
-82 kDa
XBP1s: - + - - - + + +

Sup Fig 1

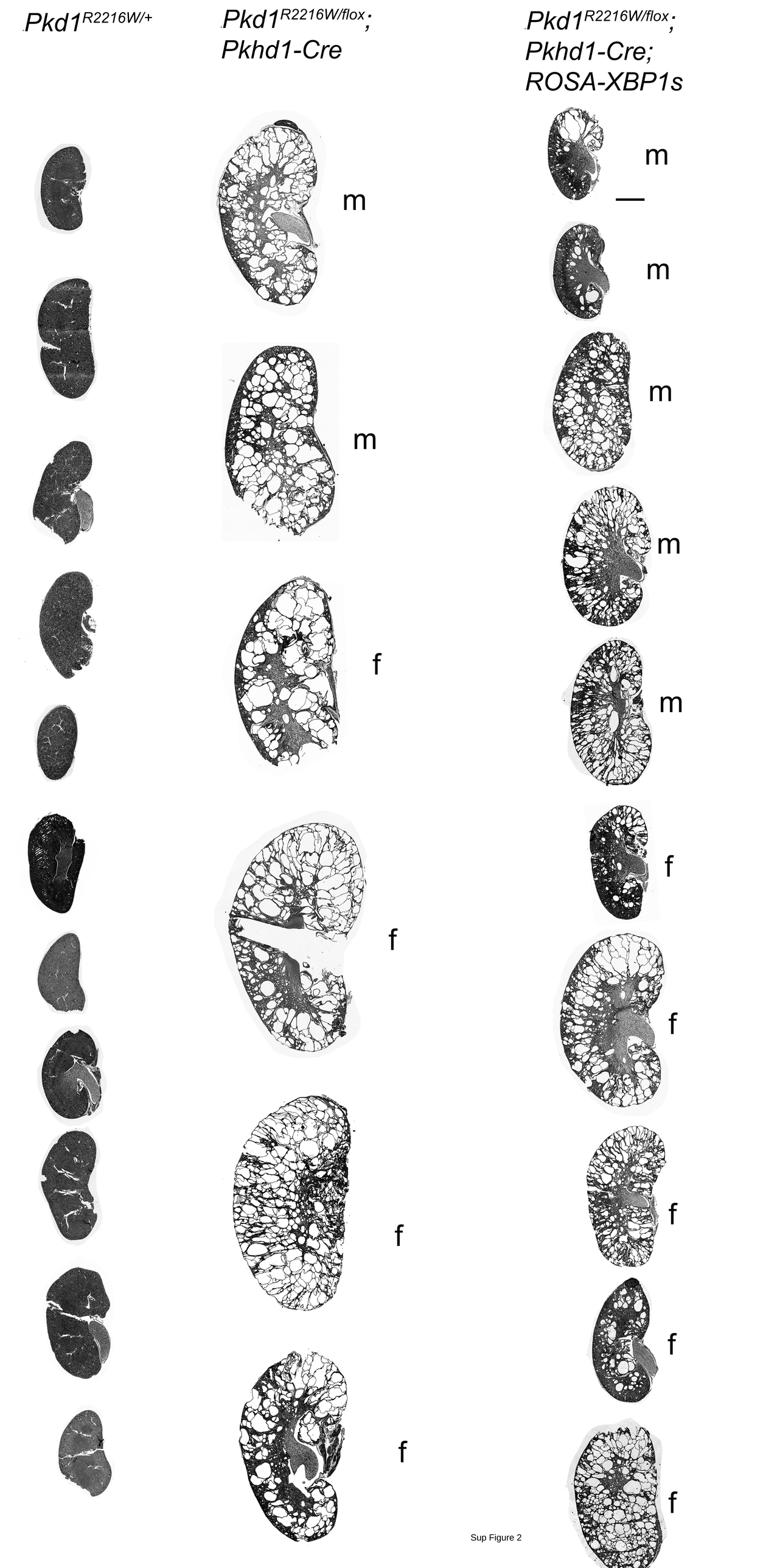
Pkd1R2216W/+
Pkd1R2216W/flox; Pkhd1-Cre
Pkd1R2216W/flox; Pkhd1-Cre; ROSA-XBP1s
m
m
m
m
f
m
m
f
f
f
f
f
f
f
f
f

Sup Figure 2

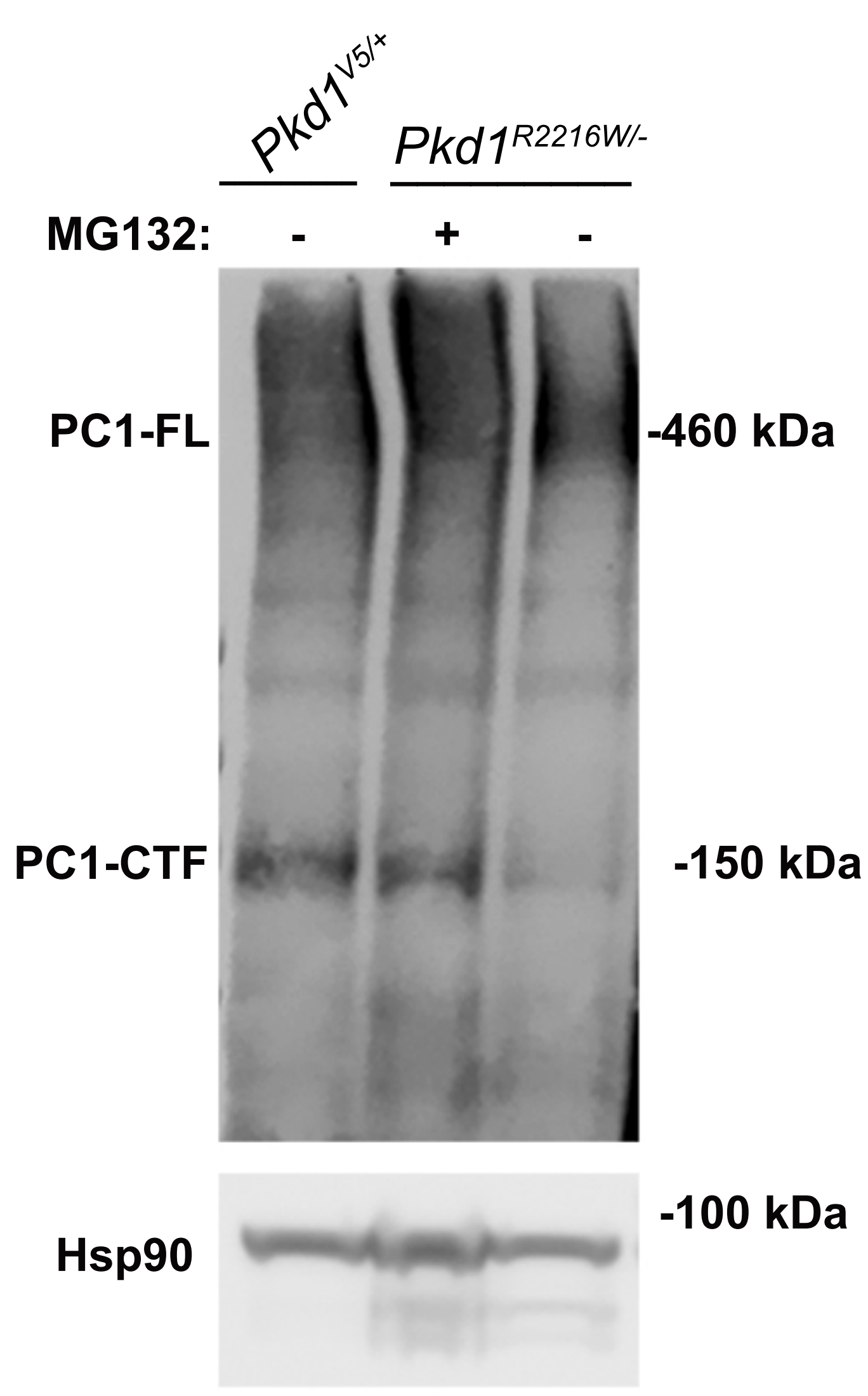
Pkd1V5/+
Pkd1R2216W/-
MG132:
-
+
-
PC1-FL
-460 kDa
PC1-CTF
-150 kDa
Hsp90
-100 kDa

Sup Figure 3

A

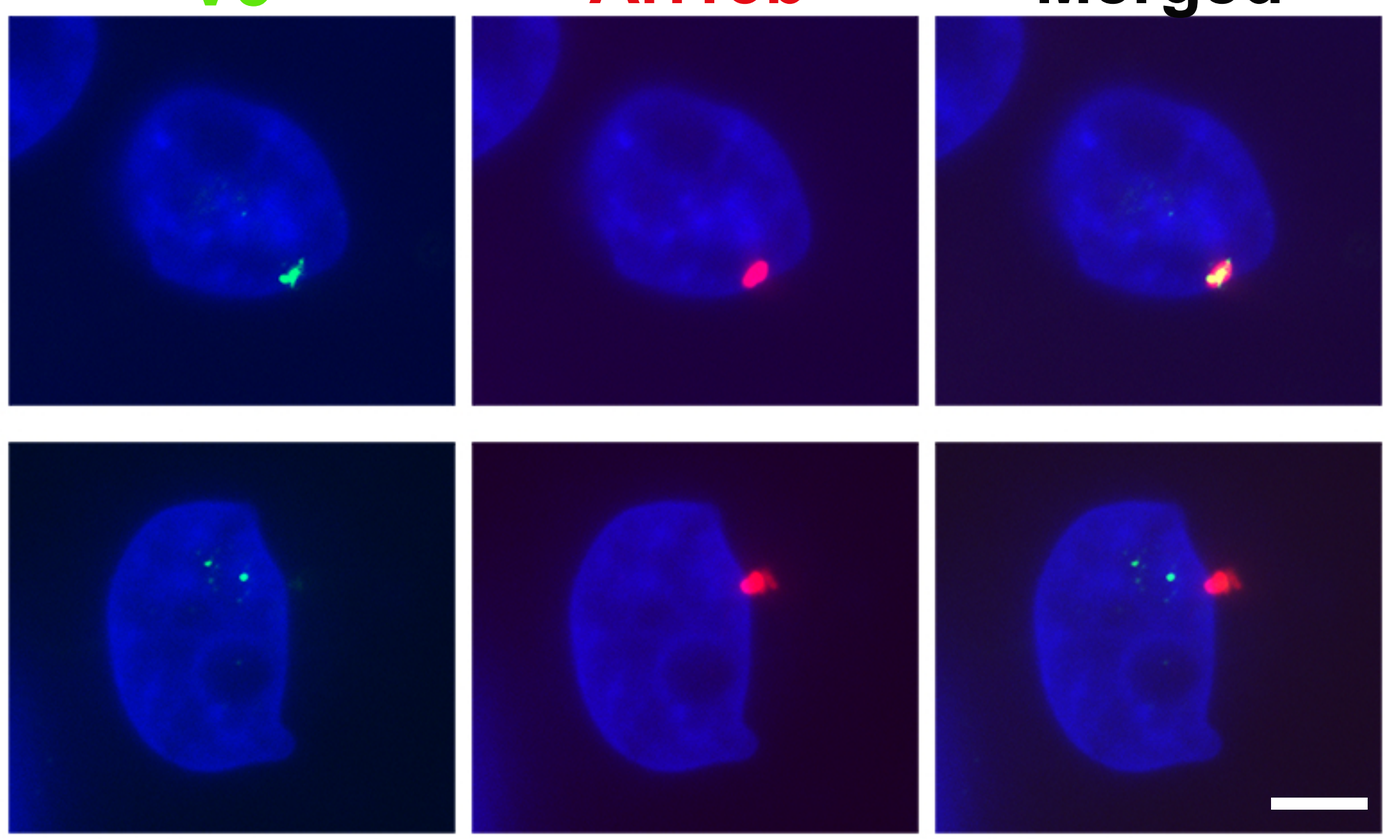

B

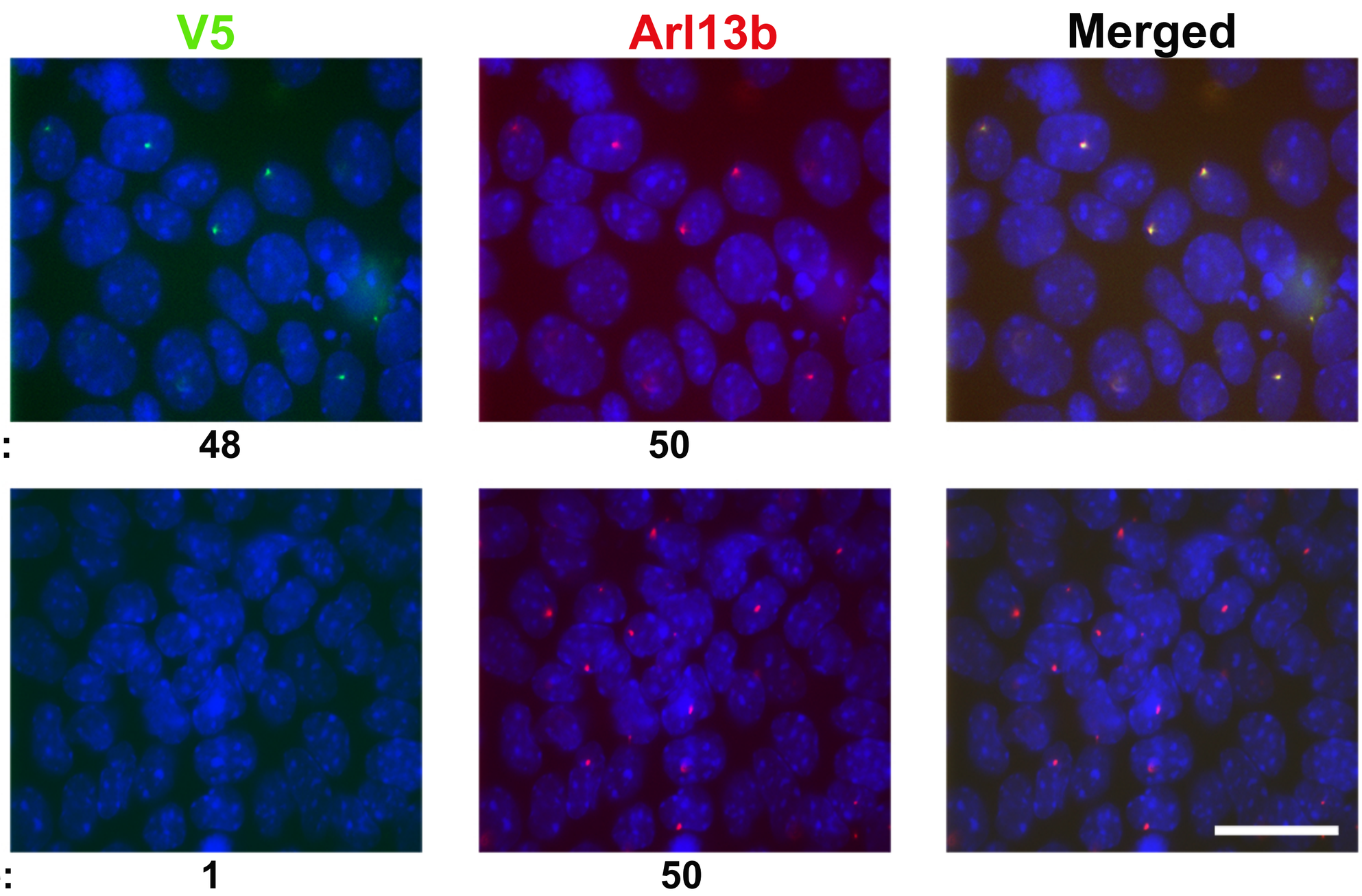

Sup Figure 4

A

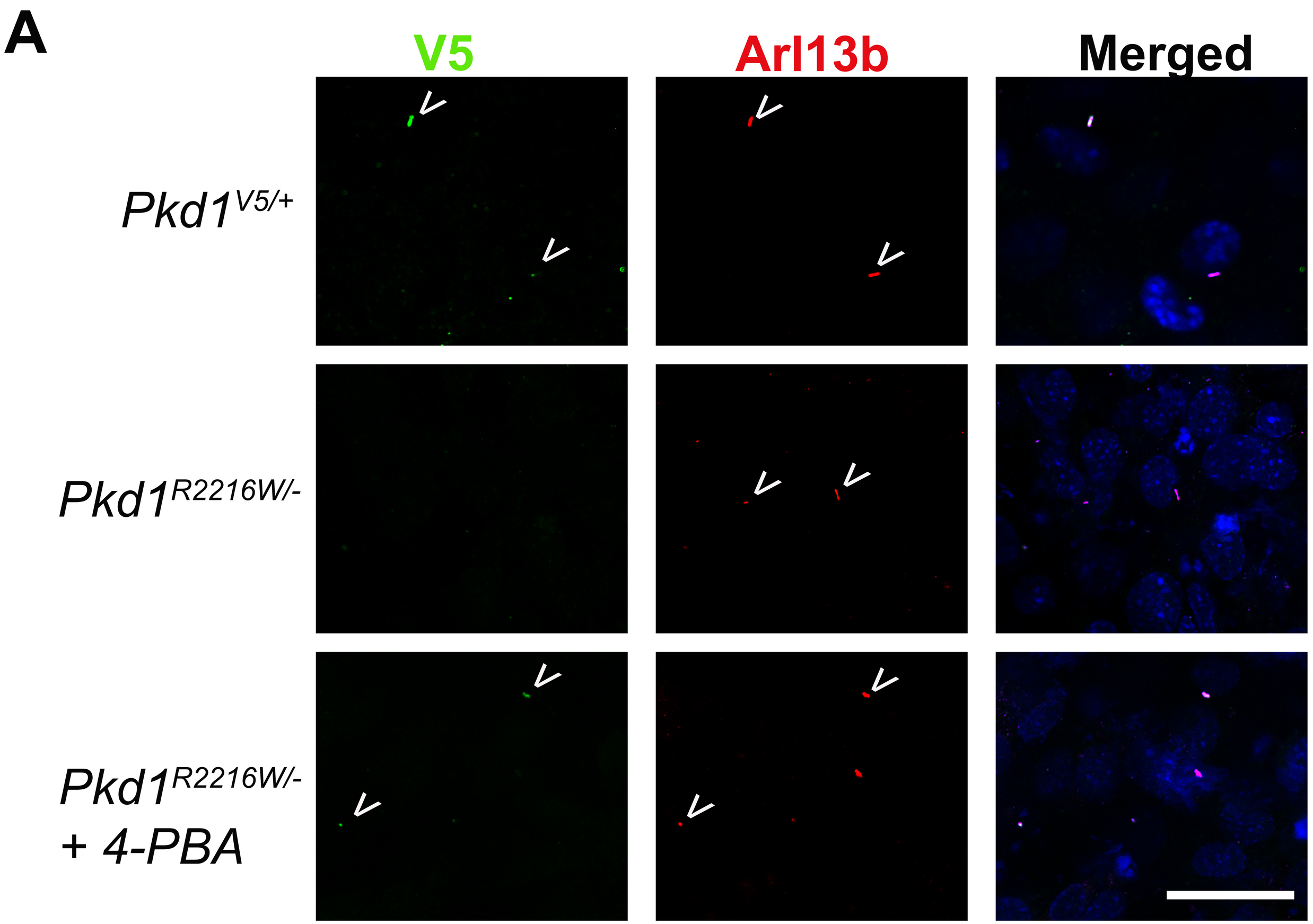

B

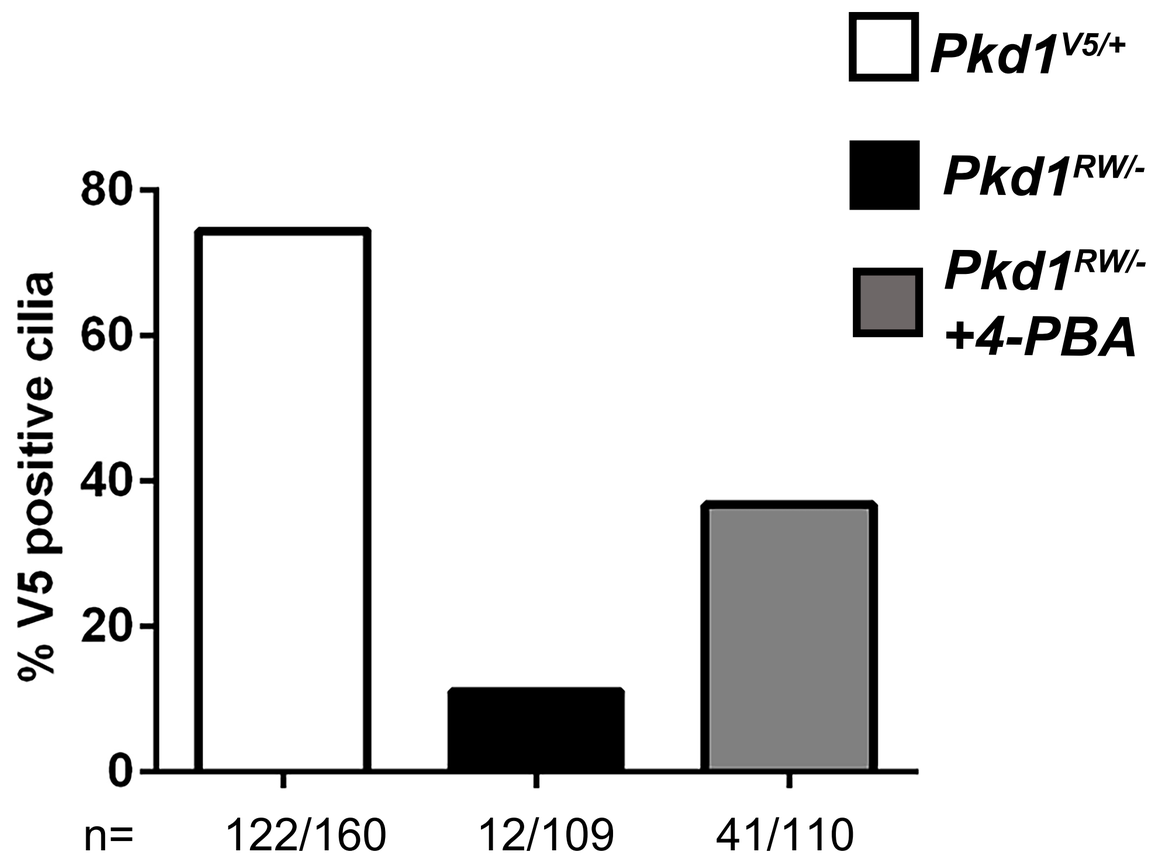

Sup Figure 5

A

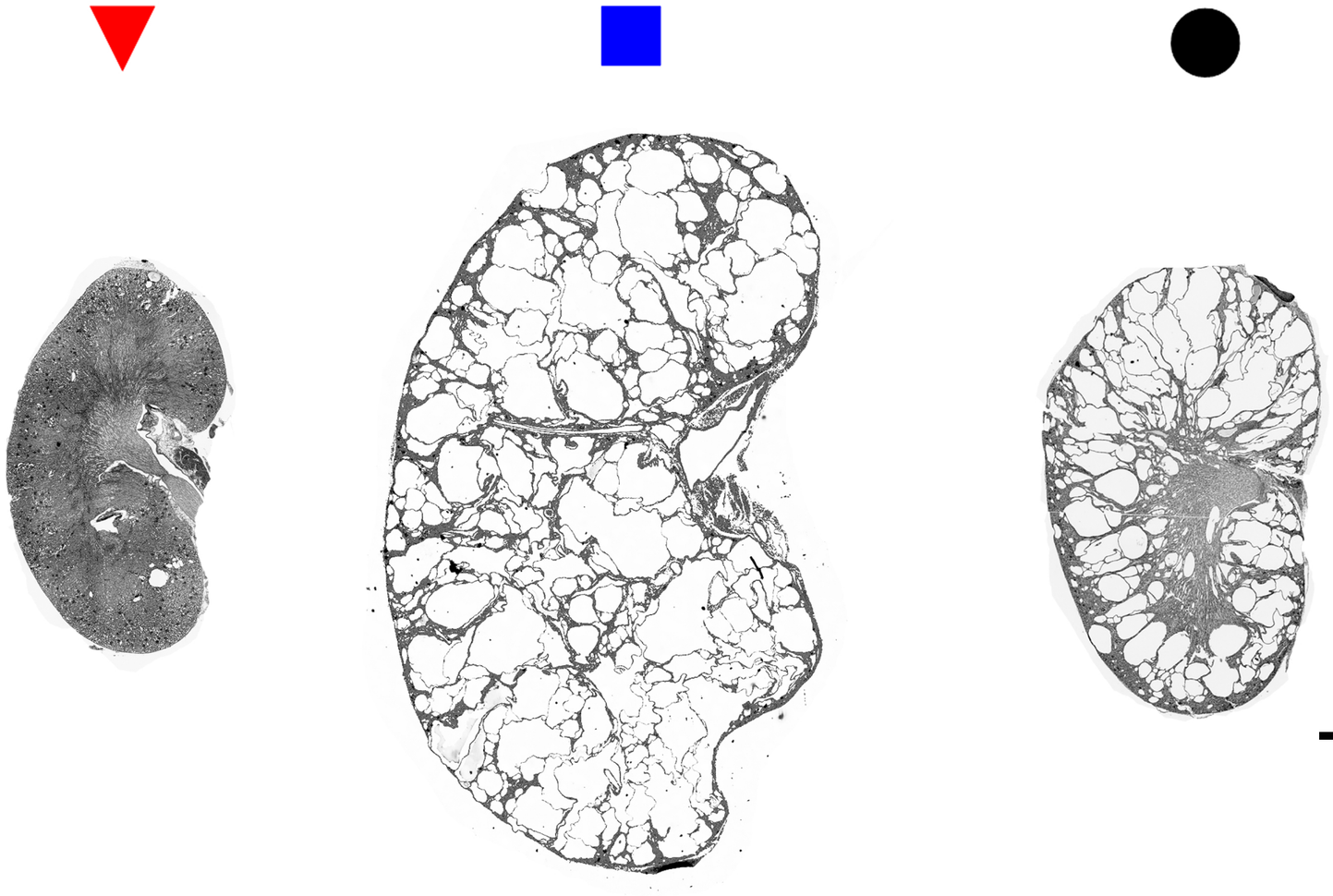

Pkd1$^{R2216W/+}$

Pkd1$^{R2216W/fl}$*; Pkhd1-Cre*

Pkd1$^{R2216W/fl}$*; Pkhd1-Cre; Pkd2-BAC*

B

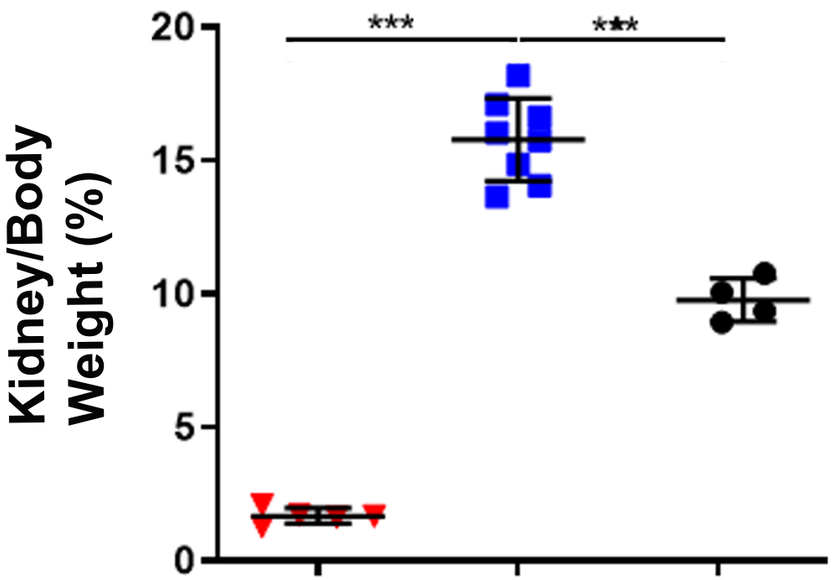

C

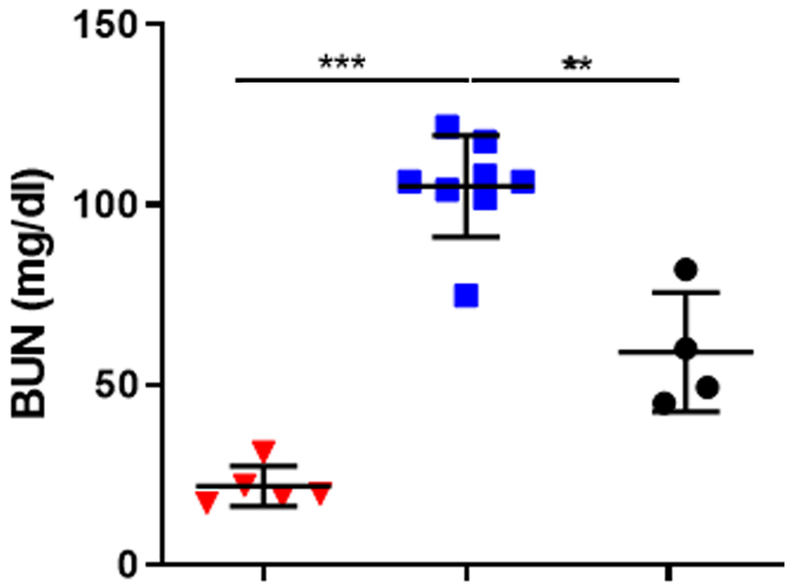

Sup Figure 6

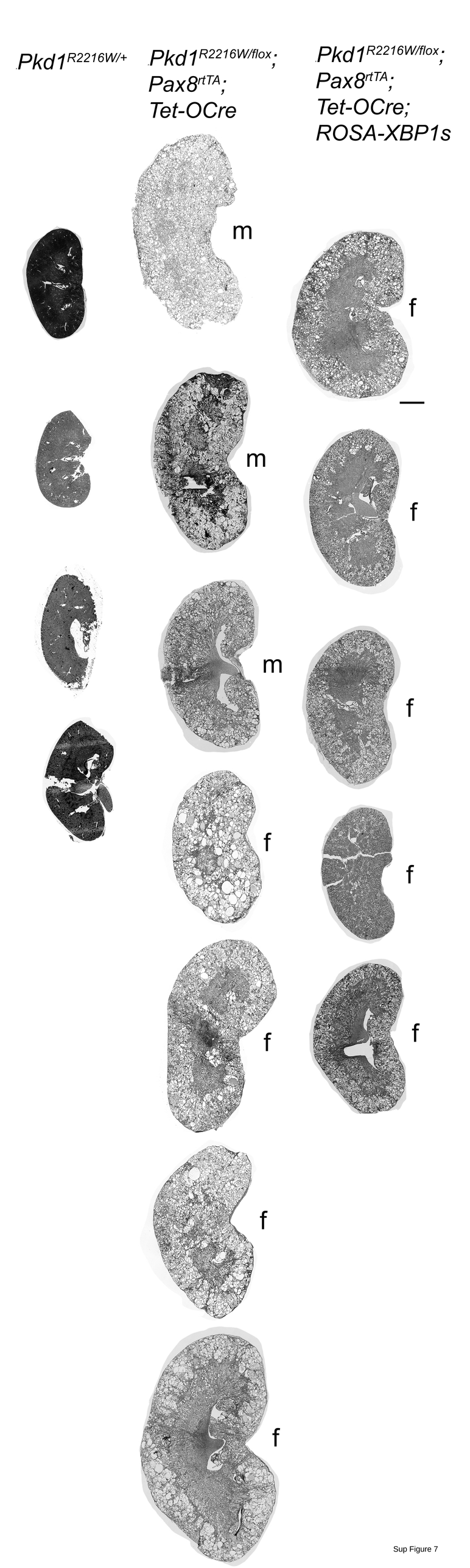
Pkd1R2216W/+
Pkd1R2216W/flox; Pax8rtTA; Tet-OCre
Pkd1R2216W/flox; Pax8rtTA; Tet-OCre; ROSA-XBP1s
m
m
m
f
f
f
f
f
f
f
f
f

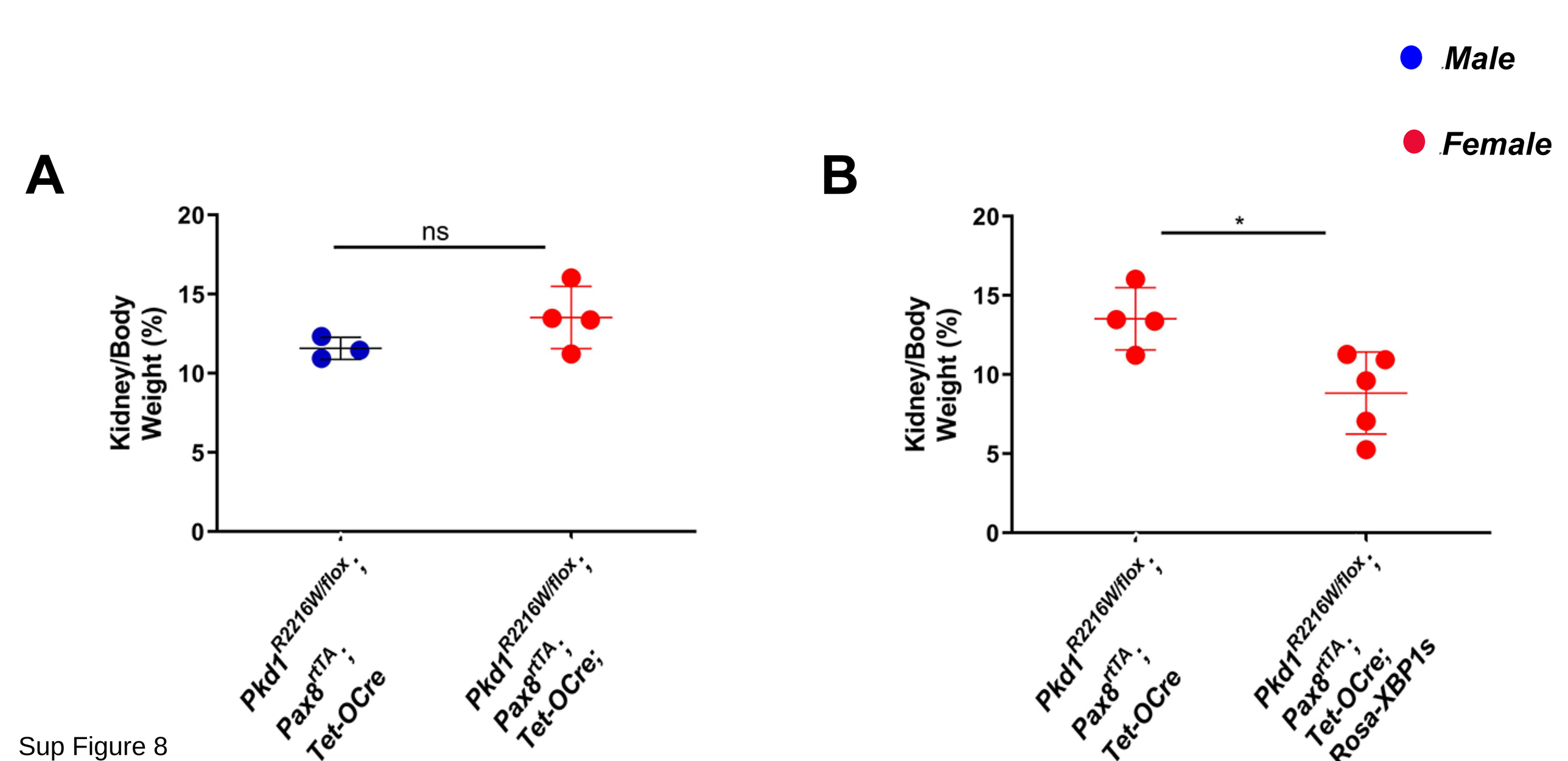
A
B
Male
Female
Kidney/Body Weight (%)
20
15
10
5
0
ns
*
Pkd1R2216W/flox ; Pax8rtTA ; Tet-OCre
Pkd1R2216W/flox ; Pax8rtTA ; Tet-OCre; Rosa-XBP1s

Sup Figure 8